

# FINITE ELEMENT ANALYSIS OF AUTOCLAVE PROCESSING OF LARGE COMPOSITE STRUCTURES USING A SUBSTRUCTURING TECHNIQUE

A. Johnston<sup>1</sup>, P. Hubert<sup>1</sup>, K. Nelson<sup>2</sup>, and A. Poursartip<sup>1</sup>

1 - Composites Group, Department of Metals and Materials Engineering,  
The University of British Columbia, Vancouver, B.C., CANADA

2 - Boeing Defense & Space Group, Seattle, WA, USA

## ABSTRACT

The full potential of composite materials in commercial aerospace applications can only be realized if the relatively high material costs are offset by exploiting their inherent suitability for direct manufacture into large monolithic structures, thereby significantly reducing production costs. However, the manufacture of such structures presents a number of difficult challenges, of which one of the most important is the prediction and control of process-induced deformation. Modelling the processing of such structures using the plate and shell elements typically employed in finite element analysis is problematic due to the very local action of most important processing phenomena. This paper discusses the application of a comprehensive 2-D finite element processing code, COMPRO, to the prediction of process-induced deformation in stiffened substructures. Predictions are compared to experimental measurements and a technique for using the substructure analysis results in a full-scale F.E. model of the complete structure is presented.

KEY WORDS: Composite Structures, Process Modelling, Warpage

## 1. INTRODUCTION

Empirical tooling and process cycle optimization techniques are unsuitable for large structures, particularly in commercial applications where low cost and rapid development times are essential. To minimize the cost and uncertainty of this phase of the design process, there is a need to implement a science-based approach to composites manufacturing.

Over the past two decades, a number of increasingly capable computational models for the processing of polymeric composite materials have been developed [e.g. 1-8]. Some of these models have focused largely on a single phenomenon such as heat transfer and resin reaction kinetics [e.g. 4,6,7], resin flow [e.g. 2], or stress development [e.g. 8,9] while others have been more broad in scope examining a number of important processing phenomena and their interactions [e.g. 1,3,5]. Currently only models by Bogetti and Gillespie [5] and White and Hahn [9] incorporate analyses of stress development *throughout* processing. While potentially very useful for research, neither model can be used for components of appreciable complexity.

## 1.1 Size Scales of Process Modelling

The scales of interest in processing and process modelling range from the level of fibre and matrix to large-scale structures (Fig. 1). The analysis of the entire structure requires large-scale or ‘global discretization’ models, employing plate and/or shell elements. However, with such models it is generally not possible to capture the effect of small-scale geometric variations (e.g. local resin flow or through-thickness effects) and mechanism interactions that are often important contributors to warpage. Between these extremes there is an intermediate ‘local discretization’ level at which it is still practical to use elements of small enough size to adequately examine the most important contributors to process-induced warpage. The challenge is to develop a practical method for transferring the predictions of such intermediate ‘local discretization’ to the ‘global discretization’ of the large structure of interest.

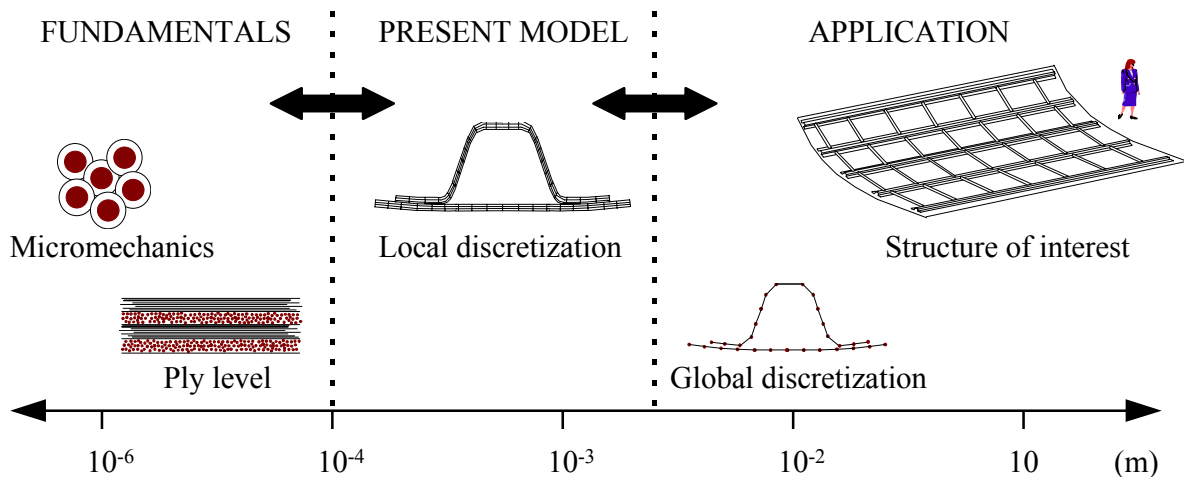


**Figure 1** Range of scales of interest in modelling the processing of composite structures (from [10])

## 1.2 Process Modelling Software

In this work we use COMPRO, a comprehensive two-dimensional finite element process modelling software developed by the Composites Group at The University of British Columbia specifically to analyze industrial autoclave processing of composite structures of intermediate size and complexity. COMPRO incorporates analyses of a number of important processing mechanisms including component internal temperature, resin degree of cure, resin flow and the development of residual stress and deformation. This commercially available software can examine complex 2-D structures with multiple composite and non-composite materials, including the effects of process tooling and autoclave characteristics. A more detailed description is given in [10].

A case study is presented to demonstrate the application of COMPRO to process-induced warpage of a large-scale composite structure by employing a substructuring method.

## 2. CASE STUDY

### 2.1 Modelling of a Large-Scale Composite Structure

As part of the product development phase for a large composite structure such as that shown in Fig. 2, finite element analyses will normally be performed to study the in-service mechanical behaviour under a variety of loading conditions. The initial conditions for such analyses will normally assume the as-designed part geometry and a nominal initial stress state, perhaps including a hygro-thermal contribution. This approach may not be adequate since there may be significant warpage and/or residual stresses induced during processing. In addition, even when warpage is small, significant pre-loads may be required to force adjacent components to fit together.

In our proposed approach, the first step in predicting the post-processing state of a large structure is to start with the same FE mesh as used in later analyses, but with a shape based on process tooling rather than the as-designed shape. If the structure is too large to be discretized fully, then an intermediate 'local discretization' must be performed.

This can often be accomplished by taking advantage of the fact that many large, complex structures, such as the one in Fig. 2, are composed of a small number of simple repeating units or substructures. In these cases, it is feasible to use small-scale models to analyze each different type of substructure individually and to use their predictions as input to the larger-scale discretization.

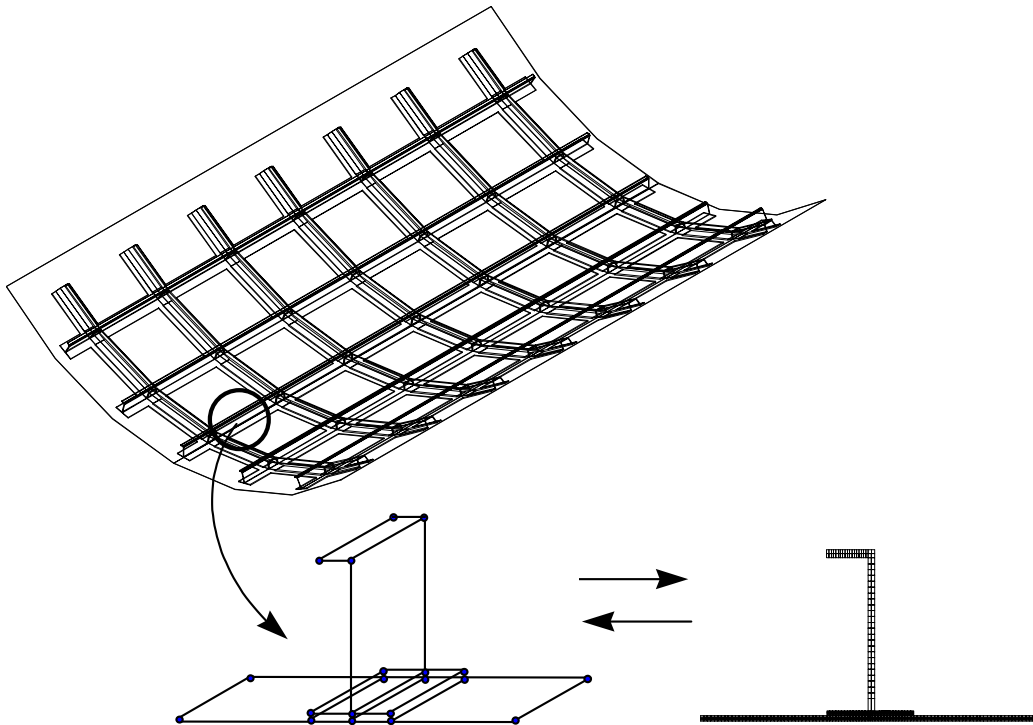


**Figure 2** A large complex structure and a typical substructure showing 3-D shell element 'global' discretization and 2-D 'local' (COMPRO) discretization

## 2.2 Representative Substructures

Substructures must be similar both in geometry and in the boundary conditions which they see during processing. Thus a substructure in the interior of the part may have to be examined separately from one on the edge, even if they have identical geometry. For our case study, as shown in Fig. 2, a local-scale finite element description of each J-frame substructure is developed and the processing boundary conditions determined.

An analysis of two typical J-stiffened substructures was performed. These substructures are illustrated in Figs. 3 and 4. The face sheets for both parts were made of 12-ply of Hercules AS4/8552 grade 190 prepreg tape with  $[45/90/-45/0/45/90]_s$  lay-up. A single pre-cured braided J-frame made by RTM was centered on the top face sheet and bonded to it using Cytec Metlbond 1515 structural adhesive, which is also used to bond the skins to the Hexcel HRP 0.1 kg/m<sup>3</sup> (8 lb/ft<sup>3</sup>) honeycomb core. No special tooling was used to prevent the frames from shifting during cure.

The parts were assembled on a large aluminum tool with a constant radius of curvature of 3.10 m (122") in the y-direction and cured using the process cycle shown in the inset in Fig. 5. To examine part-to-part variability, three samples of both components were built. As a baseline, three samples of skins and honeycomb structures with no frames were also built.

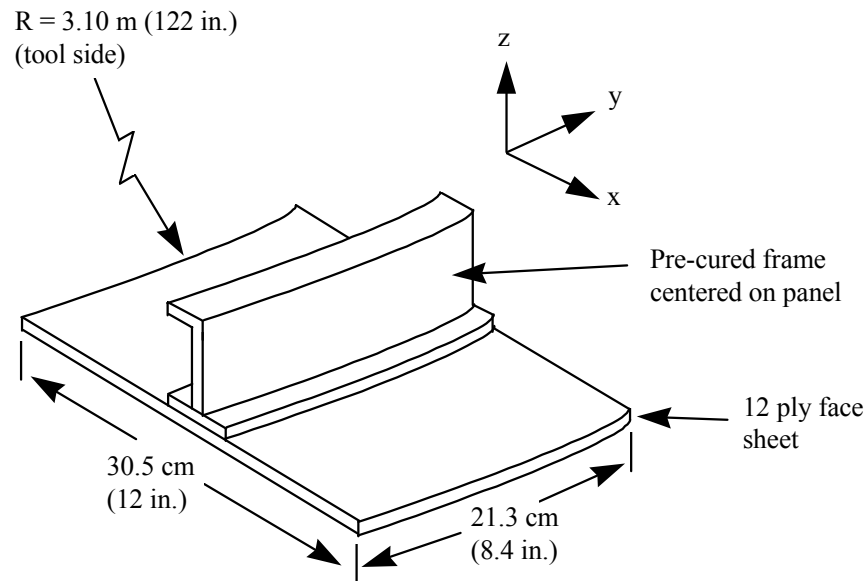


**Figure 3** Skin and J-frame Substructure

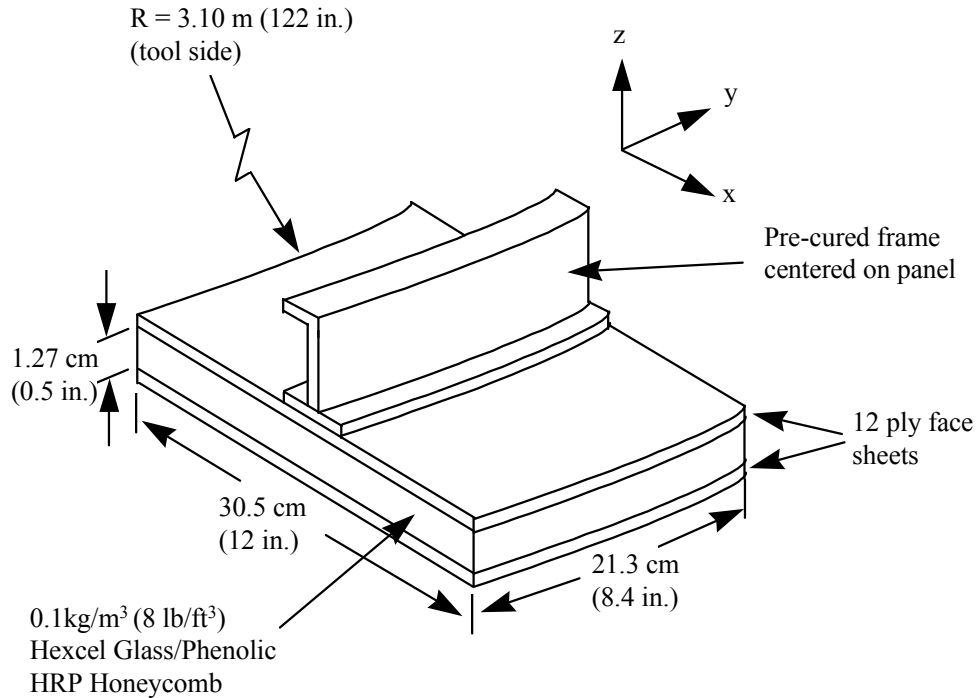


**Figure 4** Honeycomb and J-frame Substructure

### 2.3 Finite Element Modelling

Finite element descriptions of all parts were generated for COMPRO using the PATRAN preprocessor. An example of the FE discretization employed is illustrated in Fig. 5. As shown in this figure, cross-sections of the representative parts were discretized using 4-noded isoparametric plane-strain elements. A simplified, rectangular representation of the lower section of the J-frame (the 'foot') was employed in which the adhesive 'noodle' was ignored. The adhesive layer between the foot and the skin was considered, but the honeycomb/skin adhesive was not modelled. The complex geometry of the tool was replaced with a thin rectangular section with 'effective' properties chosen to mimic the actual thermal and in-plane mechanical behaviour. A 'sliding' condition was employed for the lower surface of the tool to simulate the high bending rigidity of the tool actually used. Interaction between the tool and the lower surface of the part was modelled using an elastic 'shear layer'. Flow of the matrix resin was not calculated. As illustrated in Fig. 5, a convective heat transfer boundary condition was assumed at all external model surfaces, with a heat transfer coefficient calculated from tool heating rate measurements.

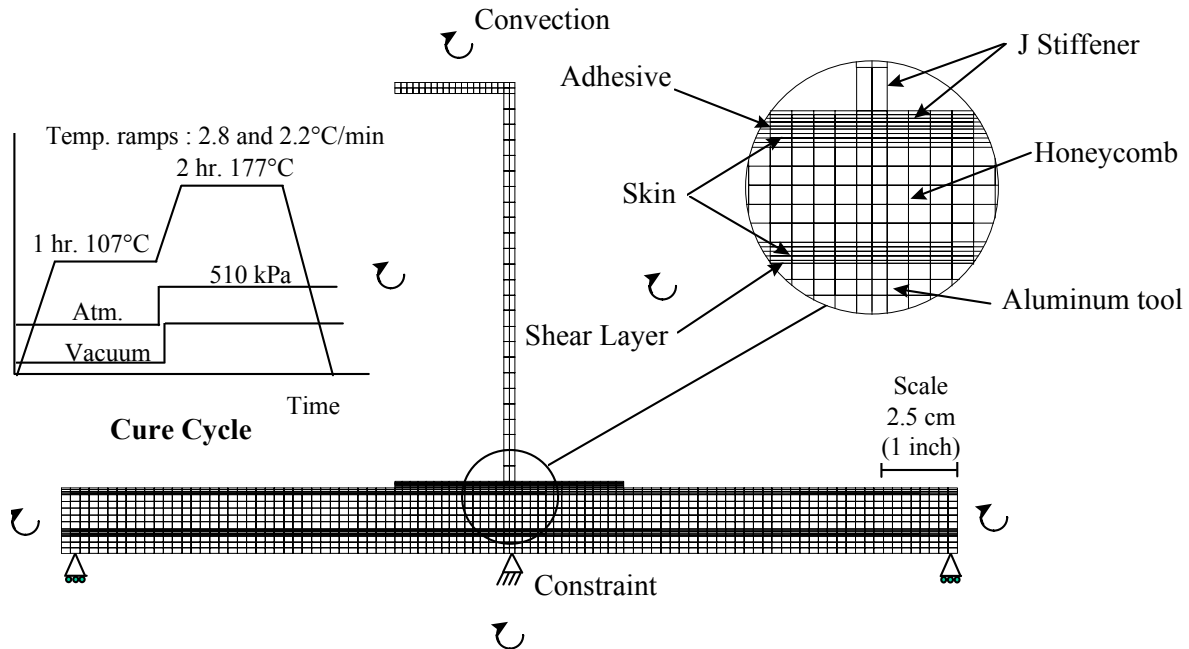


**Figure 5** Finite Element Representation of Honeycomb and J-frame Substructure

### 3. RESULTS

#### 3.1 Experimental Results

Measurements of the process-induced warpage of the representative parts were performed by comparing the components' tool-side surface profile after processing to the tool shapes (i.e. a cylinder with radius of 3.10 m). Approximately 100 points were used to map the surfaces of each component.

A typical displacement contour plot is shown in Fig. 6 for a honeycomb and J-frame substructure. The maximum deformation of this substructure was measured to be about 0.15 mm (0.006"), with both magnitude and warpage profile being very consistent for all three specimens. For comparison with the predictions, it is more convenient to plot the linear variation of the warpage with distance from the centre-line (J-frame) in the X-Z plane, as defined in Fig. 3.

The warpage of the unstiffened skin was 'outwards' (towards the tool) with a parabolic shape, as seen in Fig. 7. This shape is indicative of tool-part interaction. The warpage of the unstiffened honeycomb panel was much smaller, and barely within the limits of resolution of the measurement system, as seen in Fig. 8.

The shape of the warpage was found to be quite similar for both stiffened substructures, as seen in Figs. 9 and 10. In both cases, the tool-side surfaces warped 'inwards' (away from the tool) with warpage being approximately symmetric about the center line of the J-frame and varying approximately linearly with distance from this line. As expected, the skin and J-frame substructure exhibited a much higher level of warpage than the stiffer honeycomb and

J-frame substructure with maximum deformation averaging about 0.9 mm (0.035") for the three skin specimens.

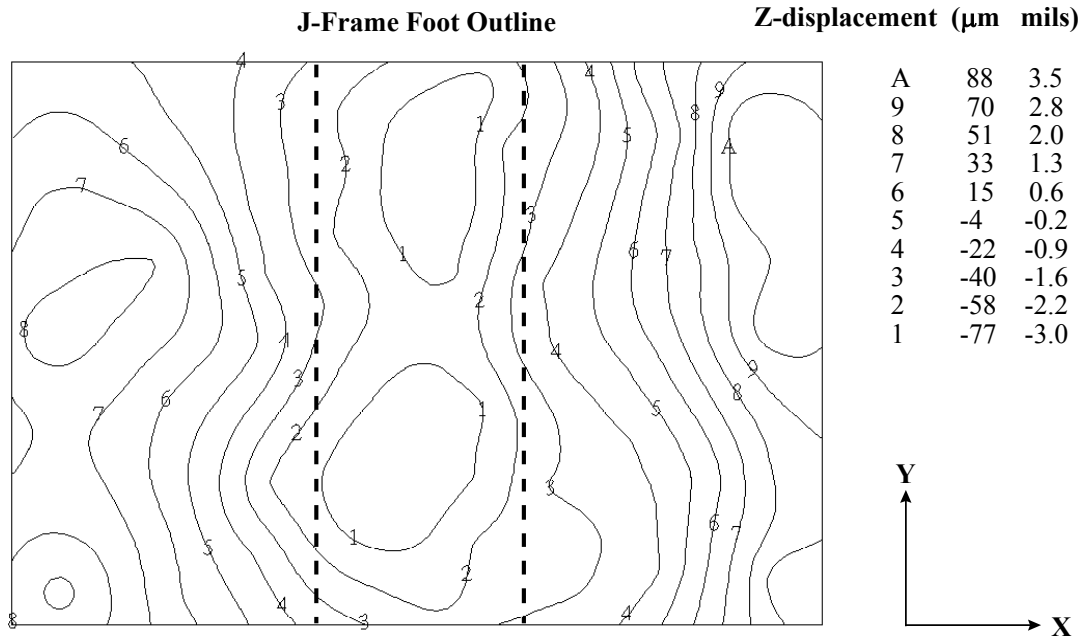


Figure 6 Typical Contour Plot of Warpage of Honeycomb and J-Frame Substructure

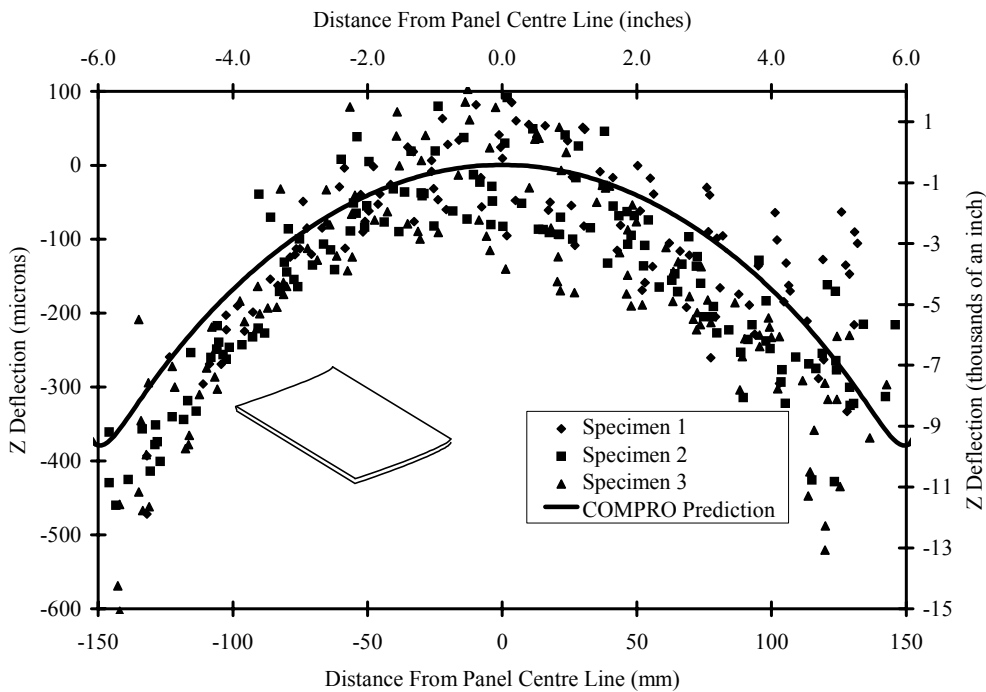
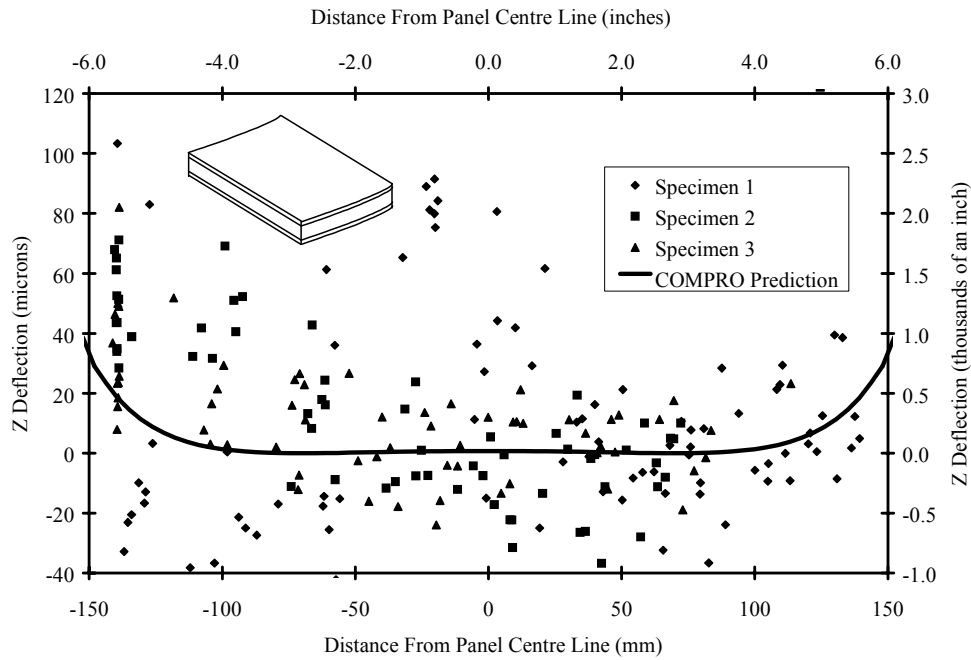
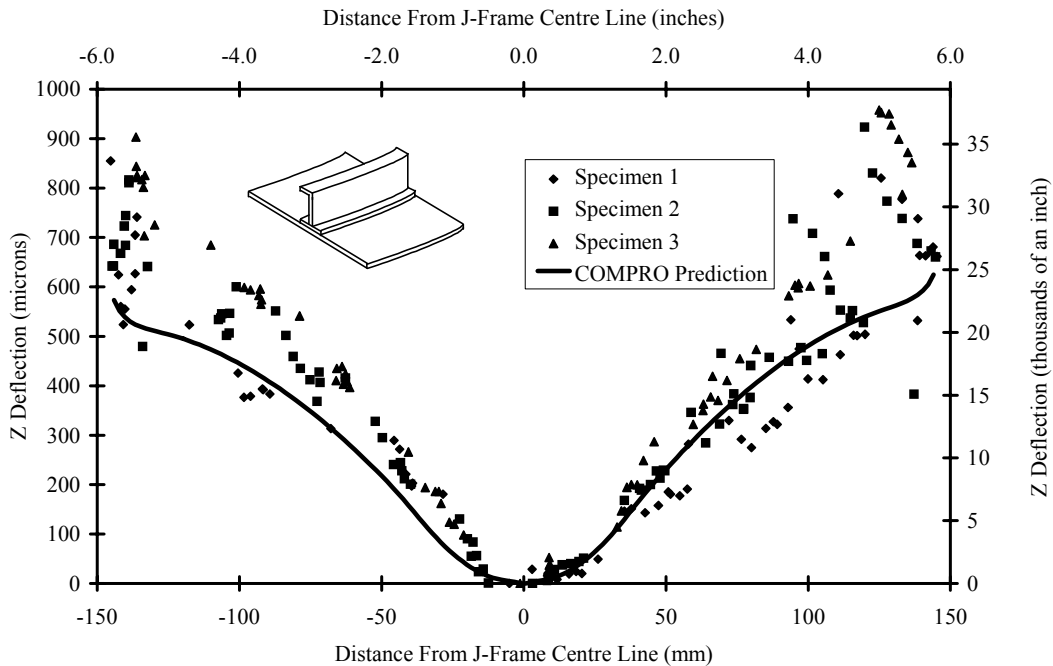


Figure 7 Warpage of Unstiffened Skin Substructure (3 specimens)



**Figure 8** Warpage of unstiffened honeycomb substructure (3 specimens)



**Figure 9** Warpage of skin and J-frame substructure (3 specimens)

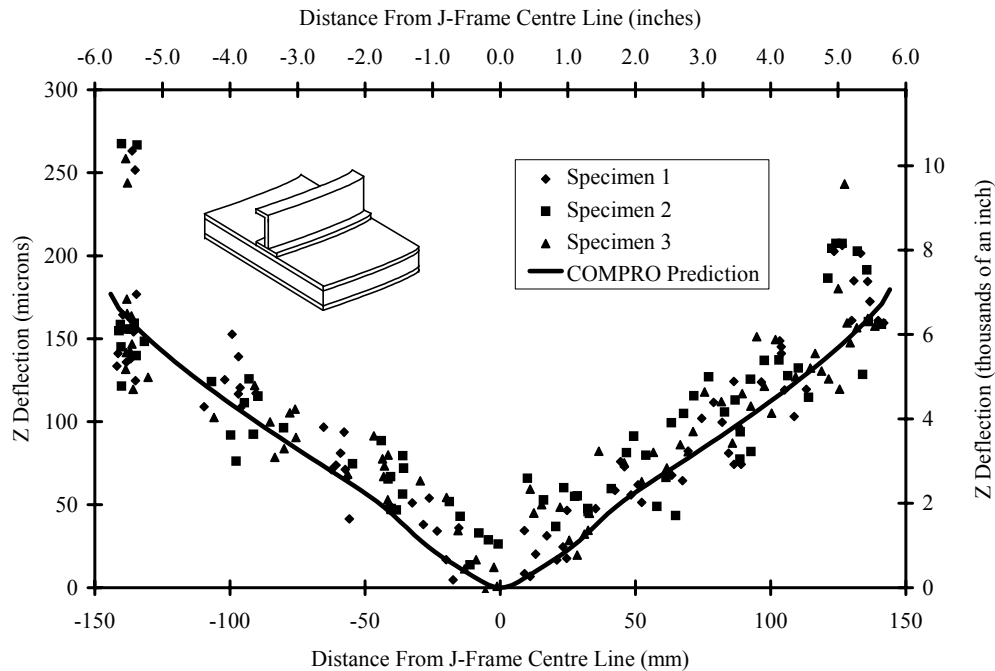


**Figure 10** Warpage of honeycomb and J-frame substructure (3 specimens)

The difference in warpage between the unstiffened and stiffened panels indicates that there are two significant sources of process-induced deformation. One is a lower face/tool interaction and the other is an interaction between the J-frame and the underlying skin. The effect of the lower face/tool interaction is to warp the panel out towards the tool. The effect of the J-frame is to pull the panels inwards and away from the tool, and in the case of the stiffened skin, the effect is large enough to change the sign of the overall warpage.

### 3.2 Model Predictions

Tool/part interaction, which can be thought of as a frictional or adhesive interaction has not been modelled previously in the literature. Although a good understanding of this mechanism is presently lacking, COMPRO allows for the effect with a thin shear layer of adjustable modulus. In the present case study, good agreement with the experimental results for the unstiffened skin substructure is found when a shear layer modulus of 1 MPa (145 psi) is used. This agreement is shown in Fig. 7, and this value of shear layer modulus is used in the rest of the case study.

Using this value of shear modulus, the warpage of the unstiffened honeycomb substructure is predicted and presented in Fig. 8. The predictions are consistent with the measurements. We do not say that the agreement is good, since the measured values are very small and at the limit of the measurement system.

The other unknowns are the properties of the adhesive and the coefficient of thermal expansion of the foot. The adhesive layer is assumed to be a resin which cures later than the prepreg material, and is found not to affect significantly the shape or magnitude of the predictions. The coefficient of thermal expansion of the foot is adjusted until there is good agreement with the skin and J-frame experiments (Fig. 9). This value is then used to predict the behaviour of the honeycomb and J-frame substructure. The predictions for this part are presented in Fig. 10 and show very good agreement with the experimental results. Since the only two unknown properties of importance were adjusted and verified with the other substructures, the good agreement that is observed in Fig. 10 is an independent verification of the validity of the approach.

#### **4. TRANSFERRING SUBSTRUCTURE PREDICTIONS TO LARGE-SCALE MODELS**

The case study presented in the previous section shows that it is possible to predict the behaviour of representative substructures. Considering the range of scales shown in Fig. 1, we now consider the transfer of the predictions from the 'local discretization' domain to the 'global discretization' domain of a larger structure. The following technique is proposed:

- The element nodes of the undeformed global model must correspond to strategically chosen positions ('reference nodes') in the undeformed local model, as shown in Fig. 11a.
- The process-induced  $u$ ,  $w$  displacements of the 'reference nodes' are determined from the local discretization model.
- Strains and curvatures (e.g.  $\epsilon$  and  $\kappa$ ) are determined such that the global element nodes see these  $u$ ,  $w$  displacements (Fig. 11b).
- In the global model, the calculated strains and curvatures are specified as element 'properties' such as thermal expansion (or other) coefficients. These strains and curvatures can then be applied by increasing the component temperature, for example, by  $\Delta T = 1$ .

Given the local reference nodes, strains and curvatures in the global model can be determined for each element using only the local finite element mesh, predicted nodal displacements, and the global element shape functions.

In the present case study, the effect of the J-frame can be isolated from the effect of the tool/part interaction and the skin/honeycomb thickness effect, and thus the procedure described above would have reasonable generality.

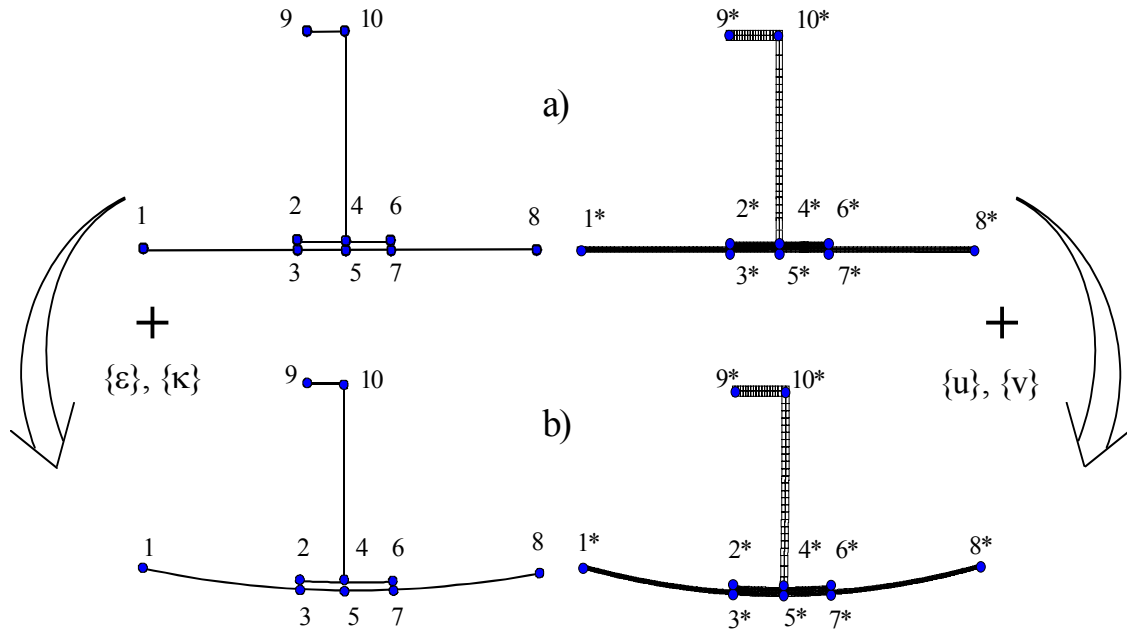


**Figure 11** The behaviour of the global model elements (left hand side) is matched to give an equivalent response to the output of the local model (right hand side)

## 5. DISCUSSION AND CONCLUSIONS

Prediction of process-induced warpage of complex composite structures requires modelling of the component in its entirety, yet computational limitations prevent modelling of large structures on a fine enough scale to capture important local effects. However, by employing the substructuring technique presented here, this task can be accomplished by modelling the processing of a small number of intermediate-scale components, then using the results in a FE model of the complete component. The processing of such intermediate-scale structures can be modelled using COMPRO, a 2-D finite element process modelling software whose application has been demonstrated with a case study.

Process modelling of composite structures, especially the large, complex structures that are the focus of this paper, offers a number of advantages over trial-and-error techniques. The final part shape may be predicted prior to construction of tooling which increases greatly in cost as structures increase in size. Then, by employing sensitivity analyses, areas of process sensitivity can be pinpointed and eliminated, resulting in much more robust manufacturing processes. Such analyses can also be used to predict process variability without requiring that a large number of components be built. Finally, by knowing the level of process-induced stresses and warpage, one may develop improved models of structural loading response and improved component design.

A number of important challenges to full implementation of the techniques outlined in this paper and Ref [10] include the fact that a large number of material properties are required by such complex modelling, many of which are difficult and expensive to obtain. Furthermore, for some mechanisms such as tool/part interaction, an adequate physical understanding and description may still need to be developed. Finally while many substructures can be

represented by 2-D models, some are likely to require 3-D models to be represented accurately.

## 6. ACKNOWLEDGMENTS

This paper summarizes work performed over a number of years under funding by the Science Council of British Columbia, the Natural Sciences and Engineering Research Council of Canada, The Boeing Company, The National Aeronautics and Space Administration and Integrated Technologies Inc. We would also like to gratefully acknowledge the significant interaction and support from our colleagues at The Boeing Company and The University of British Columbia. A special word of thanks to Mr. Robert Courdji for his help in preparing this paper.

## 7. REFERENCES

1. A.C. Loos and G.S. Springer, J. of Composite Materials, 17, (2), pp. 135-169 (1983).
2. R. Davé, J.L. Kardos and M.P. Dudukovic, Proceedings of the American Society for Composites, 1st Technical Conference, Technomic Publishing, pp. 137-153 (1986).
3. A.R. Mallow, F.R. Muncaster and F.C. Campbell, Proceedings of the American Society for Composites, Third Technical Conference, Technomic Publishing, pp. 171-186 (1988).
4. J. Mijovic and J. Wijaya, SAMPE J., 25, (2), 35-39 (1989).
5. T.A. Bogetti and J.W. Gillespie Jr., J. of Composite Materials, 26, (5), pp. 626-660 (1992).
6. T.A. Bogetti and J.W. Gillespie Jr., J. of Composite Materials, 25, (3), pp. 239-273 (1991).
7. J.M. Kenny, Proceedings of the Third Conference on Computer Aided Design in Composite Materials Technology, pp. 530-544 (1992).
8. S.R. White and H.T. Hahn, J. of Composite Materials, 26, (16), pp. 2402-2422 (1992).
9. H.T. Hahn and N.J. Pagano, J. of Composite Materials, 9, 91-108 (1975).
10. P. Hubert, A. Johnston, R. Vaziri, A. Poursartip, in A. Poursartip and K.N. Street, eds., Proceedings of The 10th International Conference on Composite Materials (ICCM-10), Woodhead Publishing, pp. 149-156, (1995).